Sea surface temperatures and environmental conditions during the "warm Pliocene" interval (~4.1–3.2 Ma) in the Eastern Mediterranean (Cyprus)

M. Athanasiou [a], I. Bouloubassi [b], A. Gogou [c], V. Klein [b], M.D. Dimiza [a], C. Parinos [c], E. Skampa [a], M.V. Triantaphyllou [a,*]

[a] Faculty of Geology and Geoenvironment, National and Kapodistrian University of Athens, Panepistimioupolis, 157 84 Athens, Greece
[b] Laboratoire d'Océanographie et du Climat: Expérimentation et Approches Numériques (LOCEAN/IPSL), Université Pierre et Marie Curie-CNRS-IRD-MNHN, 4 Place Jussieu, Case 100, 75252 Paris, Cedex 05, France
[c] Hellenic Centre for Marine Research, Institute of Oceanography, 190 13 Anavyssos, Attiki, Greece

ARTICLE INFO

ABSTRACT

Organic geochemical (alkenones) and micropaleontological (nannofossil) data from the Pissouri South section (PPS) in the island of Cyprus provided a detailed description of the paleoclimatic (sea surface temperature-SST) and paleoenvironmental conditions during the "warm Pliocene" (c. 4.1–3.25 Ma) in the Eastern Mediterranean. We found that the suite of sapropel events recorded in the studied interval took place under conditions of increased SST, enhanced water column stratification and development of a productive deep chlorophyll maximum (DCM), as witnessed by the dominance of *Florisphaera profunda* species. Such conditions are similar to those prevailing during Quaternary sapropel formation, triggered by freshwater discharges from the N. African margin due to insolation-driven intensification of the African monsoon. The absence of *F. profunda* in Pliocene sapropels from central Mediterranean records highlights the sensitive response of the eastern basin to freshwater perturbations. Comparisons between alkenone and calcareous nannofossil assemblage patterns infer *Pseudoemiliania lacunosa* as the main alkenone producer in sapropel layers; yet *Reticulofenestra* spp. contribution cannot be ruled out.

The first Pliocene alkenone-SST record in the E. Mediterranean presented here documents the "warm Pliocene" period (~4.1–3.25 Ma) characterized by mean SST of c. 26 °C. Distinct SST minima at ~3.9 Ma, 3.58 Ma and between 3.34 and 3.31 Ma, correspond to the MIS Gi16, MIS MG12 and MIS M2 global cooling episodes, before the onset of the Northern Hemisphere glaciation. Our findings imply that the peak of the MIS M2 cooling in the Eastern Mediterranean may be up to ~40 kyrs older than the age attributed before to benthic stable oxygen isotopes records of this event.

© 2017 Elsevier B.V. All rights reserved.

1. Introduction

The semi-enclosed land-locked configuration of the Eastern Mediterranean largely controls its sensitive and rapid response to climatic and environmental changes (e.g., Béthoux, 1993). It is an efficiently ventilated and highly evaporative basin with low biological production (e.g., Krom et al., 1992). In contrast to the modern oceanographic conditions, the (quasi) periodic occurrence of organic-rich layers, so-called sapropels, throughout the sedimentary record of the last 13.5 million years documents deep-water anoxic/dysoxic conditions associated with ~23 kyr precession cycle (Rossignol-Strick, 1985; Rohling and Hilgen, 1991; Hilgen et al., 2003; Lourens et al., 1996). During the

Quaternary sapropel deposition episodes, precession driven intensification of the boreal African monsoon resulted in enhanced run-off from the North African margin, notably through the Nile River discharges (e.g., Rossignol-Strick, 1985; Rohling, 1994). Increased freshwater delivery into the Mediterranean basin favored water stratification that reduced deep-water ventilation inhibiting the convective deep water formation processes. Several lines of evidence indicate that times of sapropel deposition were characterized by increased export production and improved carbon preservation under deep-sea oxygen depleted conditions (Rohling, 1994; Casford et al., 2003; Emeis et al., 2000a, 2003; De Lange et al., 2008; Rohling et al., 2015).

Besides Quaternary sapropels, the Pliocene Trubi Formation in Sicily and Southern Italy is such an example where the marly layers of the sequence (considered as the so-called sapropel equivalent) reflect the periodicity of the Earth's precession cycle (e.g., Hilgen, 1991a, 1991b;

Thunell et al., 1991a, 1991b; Lourens et al., 1996). The occurrence and timing of Pliocene sapropels has been intensively studied in the Capo Rossello Composite Section (CRCS, Sicily), the reference site for the Mediterranean basin (e.g., Lourens et al., 1992, 1996), establishing their link with orbital precession forcing and monsoon-induced hydrological changes in the Mediterranean region (e.g., Rossignol-Strick, 1985; Hilgen, 1991a, 1991b; Lourens et al., 1992, 1996).

The history of ocean temperatures during the Pliocene in the Mediterranean is so far much less constrained, mainly because reconstructions based on foraminiferal assemblages or foraminiferal stable isotope signals (e.g., Lourens et al., 1992; Lourens et al., 1996; Combourieu-Nebout et al., 2004) suffer from large limitations driven by the complex hydrology of the basin or the overprint of productivity (e.g., Lourens et al., 1996; Lourens, 2004; Becker et al., 2006;
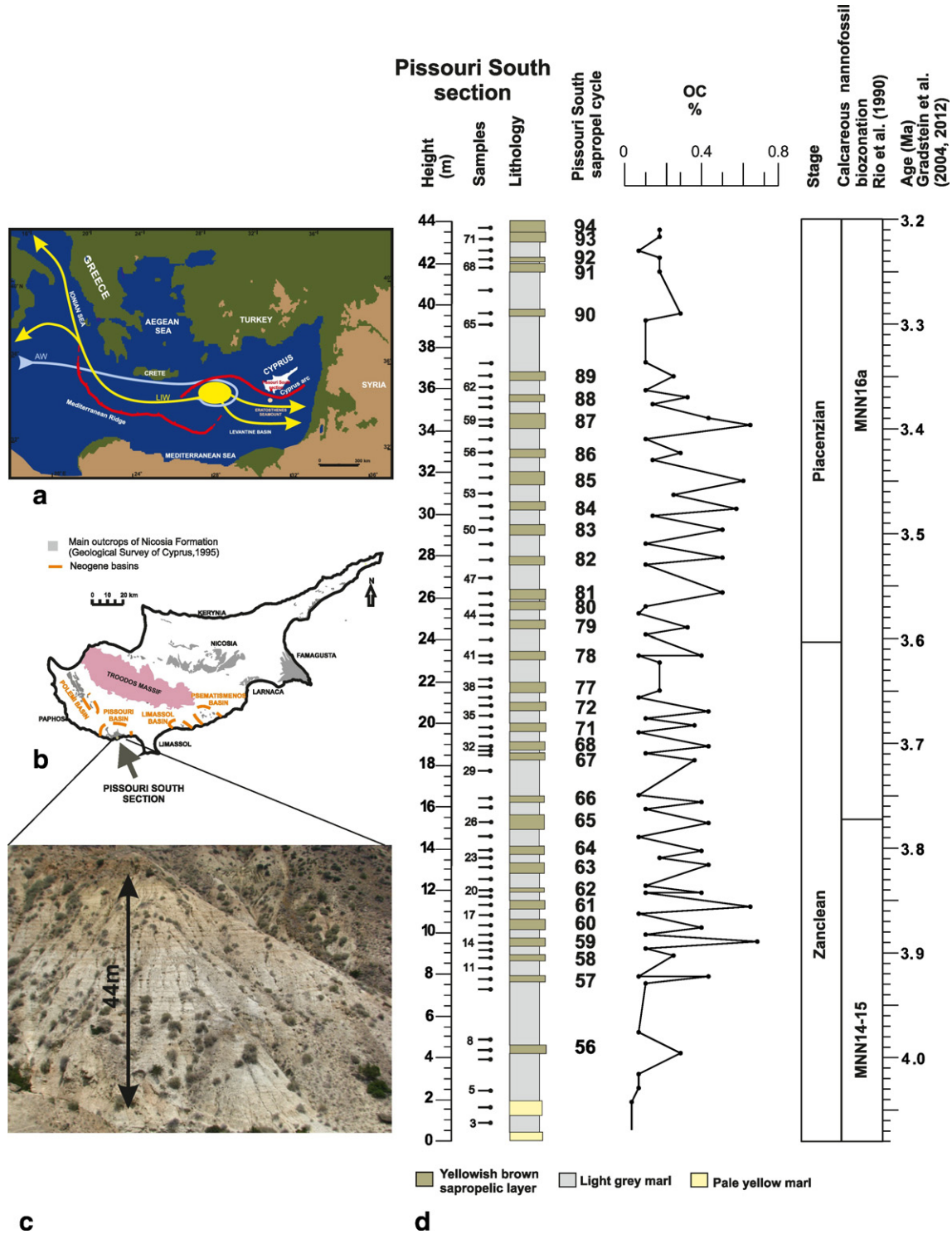

Fig. 1. a. Map of the Eastern Mediterranean; circulation patterns of Levantine Intermediate Water (LIW) and Atlantic Water (AW) are marked with yellow and blue colours respectively, red lines represent the Mediterranean Ridge and Cyprus arc, b. location of the Pissouri South section (PSS) on the island of Cyprus, c. outcrop image of the section displaying prominent lithological alternations between yellowish brown laminated layers (Lithology A) and grey marls (Lithology B), d. Sapropel cycles in PSS (after Lourens et al., 1996) and organic carbon content (OC; after Athanasiou et al., 2015).

Table 1
Organic carbon (OC), C_{37}–C_{38} alkenone and calcareous nannofossil data in sapropel layers (A) and grey marls (B) from the PSS (this study) and the CRCS (Beltran et al., 2011; Plancq et al., 2015) records.

Study area	Lithology	OC (%)	C_{37} (ng g^{-1})	C_{38} (ng g^{-1})	C_{37} (µg g^{-1} OC)	C_{38} (µg g^{-1} OC)	Accumulation rates (ng cm^{-2} yr^{-1})	F. profunda (spec. $\times 10^4$ cm^{-2} yr^{-1})
PSS (Cyprus)	A	0.39 (0.11–0.68)	404 (40.2–2006)	426 (33.4–2017)	101 (13.7–469)	107 (9.56–463)	11 (0.8–76.5)	2.858 (0.965–5.292)
	B	0.1 (0.04–0.24)	21.1 (1.75–120)	33.1 (2.11–265)	17.5 (2.63–88)	26.5 (3.41–189)	0.7 (0.02–3.7)	1.836 (1.105–2.680)
CRCS (Sicily)	A	0.11 (0.04–0.18)	40.2 (3.5–108)	45.2 (3.3–116)	36.5[a]	41.1[a]		
	B	0.04 (0.02–0.07)	3.7 (1.2–5.6)	4.1 (1.2–7)	9.25[a]	10.3[a]		
CRCS (Sicily)	A	0.6 (0.2–1.1)					12.58 (0.84–47.6)	
	B	0.33 (0.19–0.67)					1.21 (0.08–12.42)	

[a] Calculated from mean values of OC and C_{37} and C_{38} alkenones concentrations.

Colleoni et al., 2012). Moreover, diagenetic calcite precipitation (overgrowth) and salinity effects severely limit the reliable application of the Mg/Ca paleothermometry in the Mediterranean (Ferguson et al., 2008; Boussetta et al., 2011; van Raden et al., 2011). Alkenone paleothermometry, a well constrained and widely applied biomarker proxy (Brassell et al., 1986; Herbert, 2014 and references therein) appears thus as a more suitable tool for sea surface temperature reconstructions in the Mediterranean Sea. It has been successfully applied in this setting during various time frames spanning from Holocene to Eocene and especially during the Quaternary period (e.g., Emeis et al., 1998; Cacho et al., 1999; Beltran et al., 2007, 2011; Khélifi et al., 2009; Herbert et al., 2015; Plancq, 2015; Plancq et al., 2015; Tzanova et al., 2015).

Alkenones are synthesized by a small group of haptophyte algae, which in the modern ocean is restricted to two coccolithophore species of the Noelaerhabdaceae family: Emiliania huxleyi and Gephyrocapsa spp. (Marlowe et al., 1990; Volkman et al., 1980, 1995). The first occurrence of alkenones in the sedimentary record dates back to the Cretaceous (Farrimond et al., 1986; Brassell et al., 2004) and by far predates the first appearance of contemporary alkenone producers; 0.27 Ma for E. huxleyi (Thierstein et al., 1977) and 1.73 Ma for Gephyrocapsa oceanica (Lourens, 2004). Through comparisons between alkenone contents and coccolith species abundance, several members from the Noelaerhabdaceae family, such as Dictyococcites spp., Cyclicargolithus spp., Reticulofenestra spp. and Pseudoemiliania lacunosa, have been inferred as the most probable alkenone producers in sediments deposited since the Eocene (Marlowe et al., 1990; Beltran et al., 2007, 2011; Bolton et al., 2010; Plancq et al., 2012).

Numerous alkenone-SST datasets are available for Quaternary Mediterranean marine sediments (e.g., Emeis et al., 1998, 2003; Cacho et al., 2001; Gogou et al., 2007, 2016; Triantaphyllou et al., 2009; Moreno et al., 2012; Nieto-Moreno et al., 2013; Grauel et al., 2013; Rohling et al., 2002; Martrat et al., 2004). In stark contrast, there are few alkenone-based studies of Pliocene Mediterranean sections and these are limited to southern Italy and Sicily outcrops in the central Mediterranean (Beltran et al., 2007, 2011; Herbert et al., 2015; Plancq et al., 2015). Despite its sensitive response to past climate-driven perturbations and its importance as the locus of the formation of the Levantine Intermediate Water (LIW) affecting the entire basin circulation (Malanotte-Rizzoli et al., 1999; Theocharis et al., 2014), SST reconstructions are not available so far in the Eastern Mediterranean over the Pliocene.

The Late Pliocene (3.6–2.58 Ma) represents an interval in Earth"'s history during which climatic conditions are characterized by global warmth relative to today (e.g., Dowsett et al., 2013; Fedorov et al., 2013). Three short-lived cooling episodes globally recognized at c. 4.0, 3.6 and 3.3 Ma, preceded or interrupted this warm interval (e.g., De Schepper et al., 2014). The latter event took place in Marine Isotope Stage M2 (MIS M2) and represented a failed glaciation attempt within the intensification of the Northern Hemisphere Glaciation which culminated at ~2.5 Ma (e.g. Balco and Rovey, 2010; Bailey et al., 2013;

Brigham-Grette et al., 2013; Lang et al., 2016). MIS2 was followed by the Mid-Piacenzian Warm period spanning 3.3–3.0 Ma (MPWp; Dowsett and Poore, 1991), which is considered as an analogue for equilibrium climate conditions in the future if atmospheric pCO$_2$ flat lines at current levels (e.g., Dowsett et al., 2012, 2013; Seki et al., 2010; Bartoli et al., 2011; Martínez-Botí et al., 2015).

Here we present the first continuous alkenone SST record in the Eastern Mediterranean over the "warm Pliocene" (c. 4.1 to 3.25 Ma) based on analysis of the Pissouri South section on the island of Cyprus (Fig. 1). Previous studies of the PSS, based on calcareous nannofossils assemblages, have described a high resolution sapropel sedimentary sequence spanning the Zanclean/Piacenzian boundary, astronomically dated between 4.065 and 3.246 Ma (Athanasiou et al., 2015). Our alkenone-SST data extend the existing understanding of the SST evolution in the Mediterranean by c. 0.7 Ma (Beltran et al., 2007; Herbert et al., 2015; Plancq et al., 2015) and importantly, fill the gap for the understudied eastern basin. Alkenone abundance profiles are compared to nannofossil assemblage composition in order to infer putative extinct alkenone producers. We then focus on the paleoceanographic and paleoclimatic conditions, shedding light on the climate in the Mediterranean region and on the nature of global teleconnections during the "warm Pliocene".

2. Material and methods

2.1. Pissouri South section lithology and age control

The island of Cyprus in the southeastern Mediterranean basin displays well exposed Neogene sedimentary successions (e.g., Rouchy et al., 2001; Krijgsman et al., 2002; Kouwenhoven et al., 2006; Waters et al., 2010). The Pissouri South section (PSS), located at the southwestern edge of the Pissouri basin in the SW Cyprus (Figs. 1a, b), corresponds to a small NNW–SSE tectonic depression consisting of Pliocene–Pleistocene deposits of the Nicosia Formation. It is 152 m thick and comprises regular alternations of bedded marls, marly sands, silty sands and sandstones. A detailed description of the section has been provided by Athanasiou et al. (2015). The lower part of the section (first 44 m) contains 62 alternations of laminated light yellowish brown (30–60 cm thick; lithology A), and light grey marly layers (70 cm −−2.5 m thick; lithology B) (Fig. 1c, Table 1). The PSS was deposited within the calcareous nannofossil biozones MNN14–15 and MNN16a as defined by Rio et al. (1990), which span the Late Zanclean to early Piacenzian time interval. Using CRCS as a reference for the cyclochronological assessment (Lourens et al., 1996), the studied lower part of the PSS was astronomically dated between c. 4.1–3.25 Ma and comprises of the cyclical occurrence of sapropels 56 to 94 (Hilgen, 1991a) (Fig. 1d). Cyclical lithological alternations between sapropel and grey marly layers have been interpreted to represent periods of c. 21–23 kyrs assumed to reflect the Earth's orbital precession (Athanasiou et al., 2015).

A total of 72 samples were collected at an average interval of ~10 cm and ~50 cm in sapropel layers and marly deposits respectively, with an

F. profunda (%)	Reticulofenestra spp. (spec. $\times 10^4$ cm^{-2} yr^{-1})	Reticulofenestra spp. (%)	Gephyrocapsa spp. (spec. $\times 10^4$ cm^{-2} yr^{-1})	Gephyrocapsa spp. (%)	P. lacunosa (spec. $\times 10^4$ cm^{-2} yr^{-1})	P. lacunosa (%)	Reference
66.43 (38.61–89.51)	1.448 (0.103–4.026)	20.74 (0.75–72.79)	0.049 (0.000–0.133)	20.66 (0.0–17.67)	0.073 (0.008–0.163)	7.21 (0.0–30.97)	This study
16.46 (4.63–46.28)	3.528 (1.430–6.734)	52.11 (7.39–80.98)	0.463 (0.051–0.928)	15.97 (0.0–55.3)	0.122 (0.038–0.268)	3.58 (0.0–13.3)	This study
		89.8 (74.9–96.9)					Beltran et al., 2011
		92.05 (81.5–97.8)					Beltran et al., 2011
	2100	37.41 (23.32–52.4)			200	5.18 (0.19–11.6)	Plancq et al., 2015, Plancq, 2015
		32.08 (16.57–43.56)				3.07 (0.0–6.75)	Plancq et al., 2015, Plancq, 2015

average time resolution of 0.11 Ma. When possible, two samples were taken from each layer (base and top). The weathered surface layer of each sample was removed. Tectonic disturbances or vegetation cover were not observed throughout the studied part of the section.

2.2. Alkenone analysis

Freeze-dried samples (c. 20–40 g) were ground and extracted by sonication using a mixture of dichloromethane/methanol (3:1; v/v). The total lipid extract was separated into different fractions by silica gel chromatography using solvent mixtures of increasing polarity. The fractions containing the C_{37} and C_{38} alkenones were analyzed on a HP6980 PLUS series Gas chromatographer equipped with a Septum Programmable Injector and flame ionization detector on a fused silica capillary column (Chrompack CPSIL5CB, 50 m length, 0.32 mm internal diameter, 0.25 μm film thickness). Helium was used as a carrier gas at a constant flow of 2 mL/min. The oven temperature was programmed as follows: 50 °C to 140 °C (30 °C/min), 140 °C to 280 °C (20 °C/min), 280 °C to 310 °C (0.5 °C/min) and a final isothermal of 20 min.

Estimates of past sea surface temperature (SST) were made by means of the unsaturation ratio of alkenones: $[U^{k'}_{37} = (C_{37:2M}) / (C_{37:2M}) + (C_{37:3M})]$ (Brassell et al., 1986), using the global core-top calibration of Müller et al. (1998): $U^{k'}_{37} = 0.033(\text{SST}) + 0.044$, which is virtually identical to the original calibration proposed by Prahl et al. (1988). SST differences between replicate analyses were lesser than 0.6 °C. Alkenone concentrations, calculated using 5a–cholestane as internal standard, are expressed in ng g^{-1} of dry sediment, or normalized to the organic carbon content (μg g^{-1} OC). Alkenone accumulation rates (ARs) (ng cm^{-2} yr^{-1}) were calculated by multiplying the absolute alkenone content (ng g^{-1} of dry sediment) with the density of the calcite (as the main sediment constituent; 2.7 g cm^{-3}) and the estimated sedimentation rates (cm yr^{-1}) for the PSS record reported by Athanasiou et al. (2015).

2.3. Calcareous nannofossil accumulation rates

Samples were prepared following the standard smear slide techniques (Bown and Young, 1998). All samples were routinely examined at 1250×, using a LEICA DMLSP light microscope (LM); Scanning Electron Microscope (SEM) Jeol JSM 6360 (Faculty of Geology & Geoenvironment, National and Kapodistrian University of Athens) was used for preservation estimates. Species concept followed Perch-Nielsen (1985), Bown and Young (1998) and the electronic guide to the biodiversity and taxonomy of coccolithophores Nannotax 3 (ina. tmsoc.org/Nannotax3/index.html: Young et al., 2014). The results have been presented and interpreted in Athanasiou et al. (2015). The ratio between Florisphaera profunda (F), small Gephyrocapsa spp. <3 μm (sG) and small Reticulofenestra spp. <5 μm (sR, mostly R. minuta and R. minutula) abundances: $S = F/(F + sG + sR)$, (modified from Flores et al., 2000; Triantaphyllou et al., 2009) has been used as stratification index (Athanasiou et al., 2015).

In the present study a series of 30 selected samples (0.1 mg) from the prevailing lithologies of the PSS record (sapropel layers and light grey marls) have been used for the estimation of calcareous nannofossil accumulation rates so as to enhance our relative abundance data set (Athanasiou et al., 2015). After oxidation to remove the organic content (Bairbakhish et al., 1999), each sample (fraction < 32 μm) was split two into equal fractions using a McLane rotary wet splitter, filtered on Whatmann cellulose nitrate filters and dried. A piece of each filter was placed on a slide with a drop of immersion oil. Quantitative analysis of the prevailing coccolith taxa was performed by using a LEICA DMLSP polarized light optical microscope at 1250× magnification by counting forms present in four fields of view (FOV), whereas that of minor species by counting specimens present in additional six FOV. The absolute abundance of coccoliths per gr of sediment was calculated according to the following equation: N (no. of coccoliths g^{-1} sediment) = $(F \times C \times S) / (A \times W)$ where, F = filtration area (cm^2), C = number of counted coccoliths, S = split factor, A = counted area (cm^2), W = dry weight of sediment per sample (g). These values were used to estimate nannofosssil accumulation rates (ARs) (number of specimens cm^{-2} yr^{-1}).

3. Results

3.1. Alkenone concentrations

Six major alkenones were detected in all samples: heptatriacontatrien-2-one ($C_{37:3}$ Me), heptatriacontadien-2-one ($C_{37:2}$ Me), octatriacontadien-3-one ($C_{38:2}$ Et), octatriacontadien-2-one ($C_{38:2}$ Me), octatriacontatrien-3-one ($C_{38:3}$ Et), octatriacontatrien-2-one ($C_{38:3}$ Me). Their total concentrations varied over a large range (Fig. 2), from 4.03 to 4023 ng g^{-1} (6.46–932 μg g^{-1} OC), with an average of 424 ng g^{-1} (122 μg g^{-1} OC). Sapropel layers were consistently enriched (on average 830 ng g^{-1}, 208 μg g^{-1} OC; Fig. 2, Table 1) compared to the marly layers (on average 54.2 ng g^{-1}, 44 μg g^{-1} OC). PSS sapropels show higher alkenone concentrations than those recorded in Pliocene sections (c. 4.7–4.4 Ma and c. 3.6–2.6 Ma) in the CRCS southwestern Sicily outcrops (Table 1, Beltran et al., 2007, 2011). They compare to those found in Pliocene sapropels at ODP sites 967 and 969 in the Eastern Mediterranean Sea (Bouloubassi et al., 1999; Rinna et al., 2002; Menzel et al., 2003). Alkenones accumulation rates (AR) in PSS sapropels (up to 76.5 ng cm^{-2} yr^{-1}) are also higher than those reported in the CRCS (~3.6–2.6 Ma) outcrops (Plancq et al., 2015). Overall comparisons between PSS and CRCS sapropels and marly layers are given in Table 1. The overall distribution of alkenones of the PSS broadly co-varies with that of organic carbon (OC) $R^2 = 0.40$, $p < 0.001$; (Fig. 3).

3.2. Calcareous nannofossil assemblages

A detailed description of the calcareous nannofossil relative abundances from the PSS is presented by Athanasiou et al. (2015). Here we present briefly the published data (Fig. 2) in relation to the calculated accumulation rates in the present study (Fig. 2, Table 1). As shown in

Fig. 2, overall patterns/peaks co-occur in ARs and percentages of different species. *Florisphaera profunda* is the most abundant species in the sapropel layers contributing up to 90% (mean AR: 2858×10^4 ng cm^{-2} yr^{-1}; Table 1). Small *Reticulofenestra* spp. <5 μm (mainly *R. minutula* and *R. minuta*) and small *Gephyrocapsa* spp. <3 μm showed an opposite pattern dominating in the marly intervals up to 81% and 55% (mean ARs: 3.528×10^4 ng cm^{-2} yr^{-1} and 0.463×10^4 ng cm^{-2} yr^{-1}; Table 1) respectively. Stratification S-index was high up to 0.99 in the sapropel layers, while it did not exceed 0.54 in the grey marls (Fig. 2). *Pseudoemiliania lacunosa* was characterized by several abundance peaks (max. abundance 31% at ~3.82 Ma; Fig. 2) and higher ARs (mean 0.122×10^4 ng cm^{-2} yr^{-1}; Table 1) that were more pronounced within sapropels S62, S67–68, S72, S77–78 and S88–89. In addition, highest peaks of *Helicosphaera* spp. (max 6%) and *Discoaster* group (max 7.5%) have been also observed within the sapropel intervals (Fig. 2). The linear regression between total alkenones and Noelaerhabdaceae (*P. lacunosa* and *Reticulofenestra* spp.) relative abundances provided good correlation in both Zanclean and Piacenzian parts of the PSS deposits (Fig. 4).

3.3. Sea surface temperature (SST)

Apart from few exceptions alkenone SST varies between ~25 and 27.8 °C (mean 26.2 °C), attesting for warm and relatively long-term stable conditions throughout the "warm Pliocene" interval (Fig. 6a). Sapropel layers are characterized by increased SST (mean 26.6 °C) compared to the grey marly intervals (mean 25.7 °C). Three negative SST excursions are recorded within the PSS profile (Fig. 6a), marking prominent cooling events at 3.91 Ma (22.8 °C), ~3.58 Ma (22 °C) and between 3.33 and 3.31 Ma (23.2–23.7 °C).

4. Discussion

4.1. Alkenone producers during the "warm Pliocene" interval in the Eastern Mediterranean

Due to the fact that alkenones are found in sediments much older than the stratigraphic range of known extant alkenone producing coccolithophore species, comparative studies between sedimentary alkenone contents and calcareous nannofossils assemblage have been required in order to infer extinct alkenone-producers. Several species amongst Noelaerhabdaceae (*Reticulofenestra* spp., *P. lacunosa*, *Dictyococcites* spp., *Cyclicargolithus* spp.), notably *Reticulofenestra* spp. have been inferred as the most probable alkenone producers within the Cenozoic sediment record (Marlowe et al., 1990; Beltran et al., 2007, 2011; Bolton et al., 2010; Plancq, 2015).

In our Eastern Mediterranean PSS record, Noelaerhabdaceae are dominated by small *Reticulofenestra* spp. which account for up to 81% (max. 6.734 spec. $\times 10^4$ cm^{-2} yr^{-1}). They constitute, thus, a likely first-order candidate as alkenone producers, in agreement with previous data in the Pliocene sections of the CRCS-central Mediterranean (Beltran et al., 2011; Plancq, 2015) and the early findings of Marlowe et al. (1990). Nonetheless, the relative abundance of small *Reticulofenestra* spp. peaks within the low OC marly layers (52.1% and 3.528 spec. $\times 10^4$ cm^{-2} yr^{-1}, on average), whereas they display much lower values (20% and 1.448 spec. $\times 10^4$ cm^{-2} yr^{-1}, on average) within the sapropel layers (Fig. 2, Table 1). This is in sharp contrast to the pattern of alkenone concentration, which, like OC contents, maximizes within sapropels (Figs. 1, 2, 5).

Intriguingly, the pattern of *P. lacunosa* displays strong similarities with that of alkenones (Fig. 2). Its relative abundances show significant positive correlation with alkenone concentrations in both the Zanclean and Piacenzian time intervals of the PSS record ($R^2 = 0.52$ and 0.31 respectively, $p < 0.001$), suggesting a probable alkenone producer (Fig. 4). Although little is known about *P. lacunosa* ecological preferences, it belongs to placolith-bearing taxa, which in the modern assemblages are adapted to eutrophic conditions (Young, 1994). The significantly higher abundance and stronger fluctuations of the species in the Eastern Mediterranean Mid-Pleistocene interstadials suggest possible relation with higher variability in salinity and nutrient content during warm intervals (Ocean Drilling Project Site 967; Marino et al., 2008). Increased abundances of *P. lacunosa* have been previously reported in Pliocene sapropel layers implying affinities to warm stratified superficial waters (Negri et al., 2003). Furthermore, Beltran et al. (2007) pointed *P. lacunosa* as a significant contributor to nannofossil assemblages of CRCS Piacenzian sapropels (3.0–2.9 Ma). This adds circumstantial evidence for potential contribution of this species to the alkenone production. It is noteworthy that our PSS data place the first occurrence of *P. lacunosa* earlier (at least at 4.1 Ma) than data from other ocean basins (3.70–3.92 Ma, http://ina.tmsoc.org/Nannotax3; Backman et al., 2012); this is in line with existing, yet scattered, observations from early Pliocene Mediterranean sequences (Dermitzakis and Theodoridis, 1978; Driever, 1988; Lancis et al., 2015).

Even though *Reticulofenestra* spp. show weaker correlation with alkenones ($R^2 = 0.25$ and 0.05 respectively, $p < 0.001$) its possible contribution to the alkenone production cannot be ruled out, particularly within the marly layers of PSS. Actually, a slightly increased fit ($R^2 = 0.30$, $p < 0.0001$) is obtained when sapropel samples are not considered. *Reticulofenestra* spp. have been inferred as alkenone producers in Pliocene CRCS sediments (Beltran et al., 2011; Plancq, 2015). Any attempt to infer the past biological sources of alkenones is inevitably based on the assumption that the combined alkenone abundance and calcareous nannofossils assemblage's composition preserved in the sedimentary record reliably reflect their original producing abundance variations. Nevertheless, several factors may bias this relationship, such as selective dissolution and/or differential preservation-diagenetic effects and degradation process (e.g., Prahl et al., 1989; Malinverno et al., 2008), different preservation of the calcite of coccoliths compared to alkenones, possible contribution from non-calcifying species (Beltran et al., 2011; Plancq, 2015).

Based on previous studies (Conte et al., 2006; Beltran et al., 2011; Plancq et al., 2015) we assume hereafter that the potential bias on Pliocene alkenone based SST estimates due to possible genetic differences between modern and Pliocene alkenone producers is of «second order». In fact, a series of studies on both molecular (Fujiwara et al., 2001; Sáez et al., 2004; Beltran et al., 2011) and micropaleontological data (Marlowe et al., 1990; Young, 1990, 1998; Bown and Young, 1997) showed that evolutionary relationships between the modern alkenone producers and their Cenozoic ancestors are very close, with genetically-related factors having little impact on the alkenone unsaturation (Müller et al., 1997, 1998; Villanueva et al., 2002; Conte et al., 2006).

4.2. Environmental conditions associated to "warm Pliocene" sapropel deposition

The alkenone- and OC-enriched sapropel layers deposited over the c. 4.1 to 3.25 Ma interval show highest percentages of *F. profunda* (up to 90%; Figs. 2, 5), a typical Deep Chlorophyll Maximum (DCM) indicator (e.g., Okada and Honjo, 1973; Molfino and McIntyre, 1990; Castradori, 1993, 1998; Beaufort et al., 2001; Triantaphyllou et al., 2009, 2014, 2016; Grelaud et al., 2012; Athanasiou et al., 2015). This provides evidence for a productive lower photic zone associated with enhanced water-column stratification and shoaling of the pycnocline/nutricline into the photic zone (e.g., for extensive analysis see Rohling and Gieskes, 1989; Rohling, 1994; Rohling et al., 2015).

The concomitant positive excursions of *Helicosphaera* spp. and *Discoaster* spp. (Figs. 2, 5) argue for surface water freshening (*Helicosphaera* spp.; e.g., Ziveri et al., 2004; Triantaphyllou et al., 2009) and productive lower photic zone (implications for similar to *F. profunda* ecological preference of *Discoaster* spp.; Castradori, 1998; Flores et al., 2005), further supporting increased water column stratification. Such combined changes in the hydrology and nutricline dynamics of the Eastern Mediterranean have been largely documented in Quaternary sapropels (mainly S1 and S5, e.g., Bouloubassi et al., 1999;
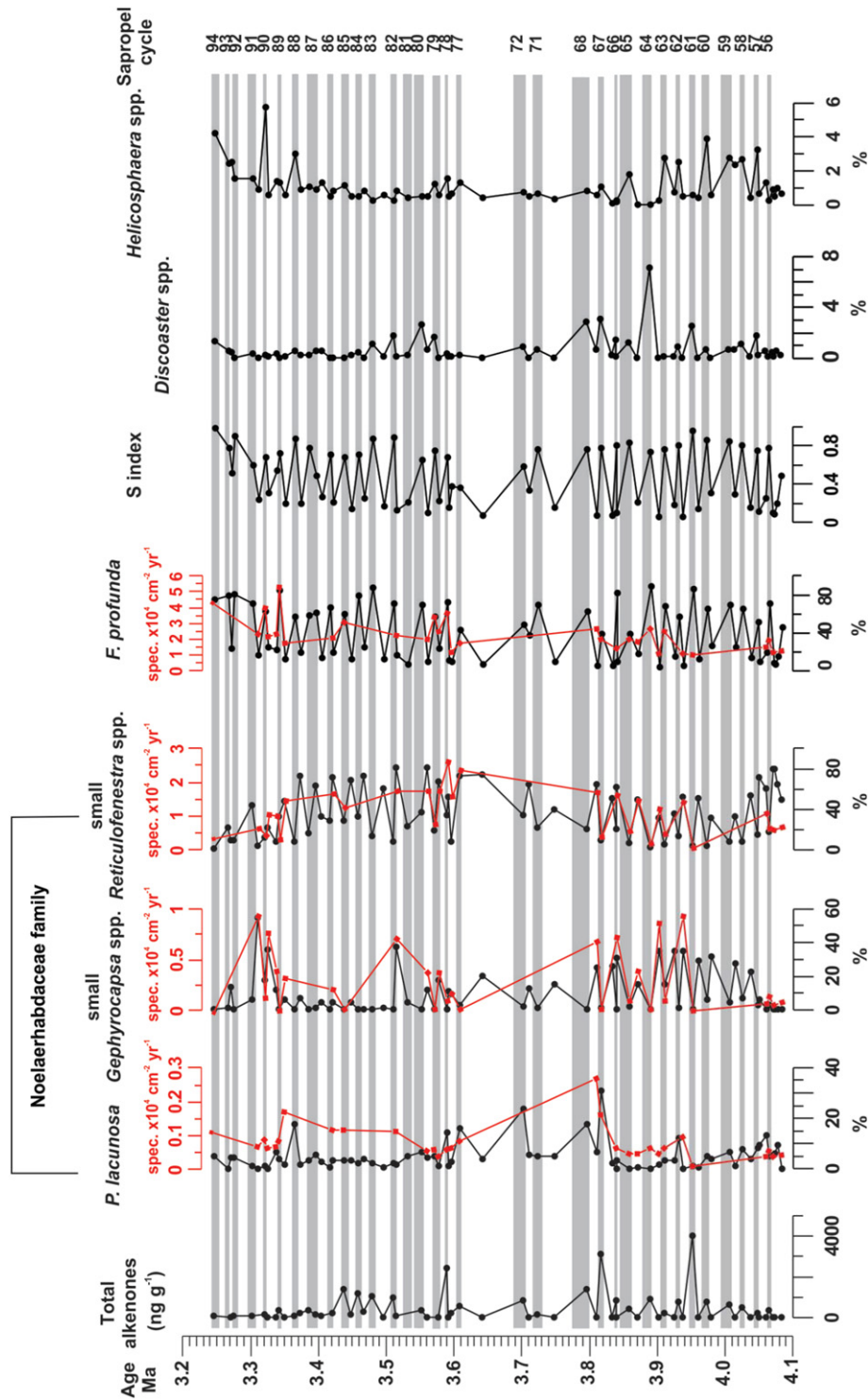
Fig. 2. Total alkenone concentrations, distributional patterns (after Athanasiou et al., 2015) and ARs (red curves, this study) of the major calcareous nannofossil and stratification index (S-index; for definition see text) in the PSS sedimentary record. Sapropel layers are highlighted in grey bands; Sapropel cycles as in Fig. 1.

Rohling et al., 2002, 2015; Triantaphyllou et al., 2009, 2010; Triantaphyllou, 2014; Grelaud et al., 2012). They are induced by precession-controlled monsoon flooding from the N. African borderland (mainly from the Nile River) that ultimately pace sapropel deposition, as first proposed by Rossignol-Strick (1985); see also reviews by Rohling (1994) and Rohling et al. (2015).

Opposed to sapropel layers, the marly alternations of the PSS show lower OC and alkenone concentrations (Figs. 1, 6). The dominance of

small placoliths (small *Reticulofenestra* spp. and small *Gephyrocapsa* spp.) points to mesotrophic-eutrophic conditions during mixing of surface waters (e.g., Gartner et al., 1987; Gartner, 1988; Takahashi and Okada, 2000; Colmenero-Hidalgo et al., 2004; Flores et al., 2005).

There has been a long-standing debate whether increase of marine export productivity or enhanced preservation of organic carbon under dysoxic/anoxic deep-water conditions or at the seafloor, led to the formation of Quaternary sapropels, although these two views are not
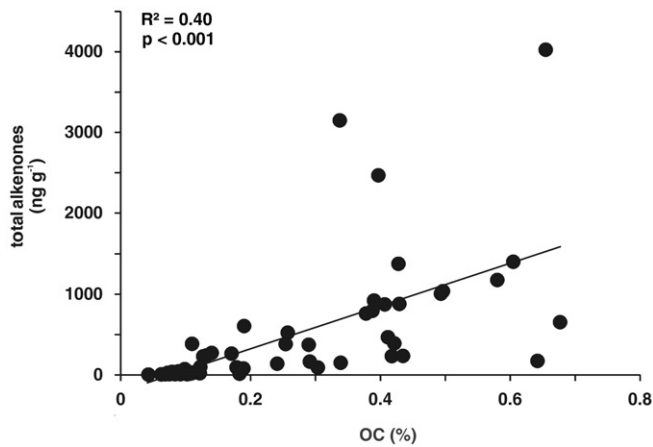
Fig. 3. Linear regression between organic carbon content and total alkenone concentration.

necessarily mutually exclusive (see reviews by Rohling, 1994; Rohling et al., 2015 and references therein). A productive lower photic zone would promote efficient export of organic matter that may undergo lesser degradation under deep-water oxygen depletion (stratified, stagnant conditions).

The striking absence of *F. profunda* in Pliocene sapropels from the CRCS in Sicily (Beltran et al., 2011; Plancq et al., 2015) and the lower alkenone and OC contents compared to the PSS record, underscores significant differences between the western and Eastern Mediterranean basins at times of sapropel deposition (e.g., Rohling, 1994; Bouloubassi et al., 1998; Stratford et al., 2000; Casford et al., 2003; Menzel et al., 2002; Menzel et al., 2003; Beltran et al., 2007; Rohling et al., 2015). In the Eastern Mediterranean, shoaling of the pycnocline/nutricline and the presence of LIW at shallow depths (compared to the Western Mediterranean) favored injection of nutrients (see Grelaud et al., 2012) and enhanced productivity in the lower photic zone (DCM), especially in areas under the strong influence of LIW, as in the case of the PSS record. Pliocene (early Zanclean) sapropels from marine cores at ODP sites 967 and 969 (close to the LIW formation zone and our study area) also show intense DCM signal (high abundance of *F. profunda* (Castradori, 1998). Moreover, compared to the western basin the Eastern Mediterranean is more sensitive to the development of deep-water anoxia due to different processes in the efficiency of deep-water renewal (e.g., Rohling, 1994; Myers et al., 1998; Bouloubassi et al., 1999; Stratford et al., 2000; Cacho et al., 2001; Rohling et al., 2015). This further favors preservation of exported organic fluxes during sapropel deposition.

Shoaling of the pycnocline/nutricline in the central Mediterranean during times of Pliocene sapropel formation, apparently did not reach the base of the euphotic layer or subsurface waters were not enough nutrient enriched to support a productive lower photic zone (absence of *F. profunda*), even in the case when stratification is proposed as the main driving mechanism (3.1–2.8 Ma; Plancq et al., 2015).

Hence, the mechanism of both Pliocene and Quaternary sapropel formation in the Eastern Mediterranean appears to be similar, involving enhanced stratification associated with a productive lower photic zone and dysoxic/anoxic conditions in the deep water layers favoring organic matter preservation (e.g., Rohling, 1994; Emeis et al., 2000b; De Lange et al., 2008). It is driven by the ~23 kyr precession cycle and the associated enhanced African monsoonal activity that pertubate freshwater discharge into the basin (Rossignol-Strick, 1985; Rohling and Hilgen, 1991; Hilgen et al., 2003; Lourens et al., 1996).

4.3. SST record and paleoclimate during "warm Pliocene" in the Eastern Mediterranean

Available SST data from Pliocene Mediterranean sections are so far limited to the central Mediterranean (Sicily) and span distinct time
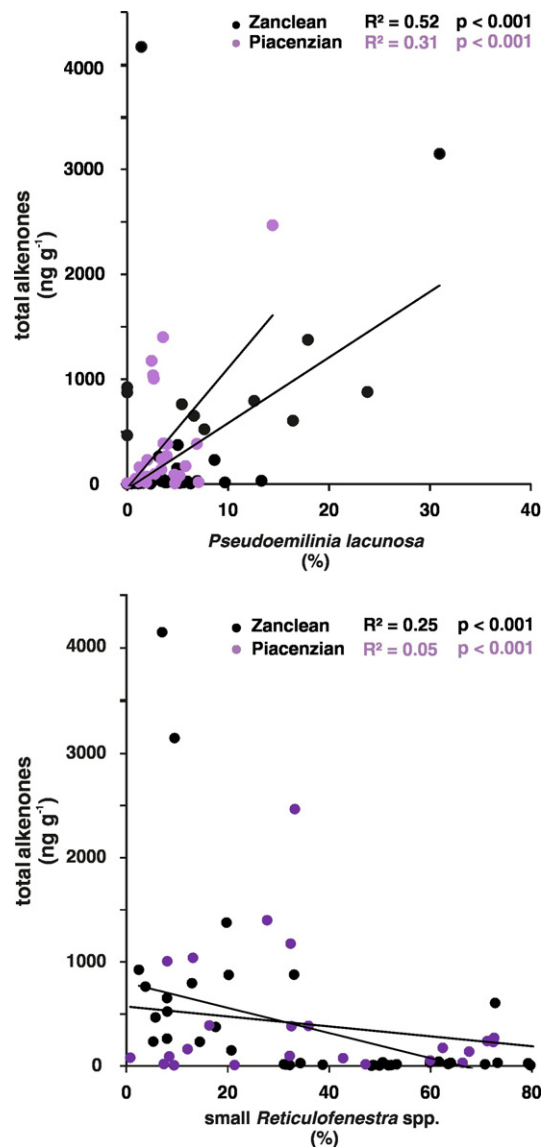

Fig. 4. Linear regression between total alkenone concentration and Noelaerhabdaceae representatives (*P. lacunosa*, small *Reticulofenestra* spp.) during the Zanclean and Piacenzian time intervals.

frames (Beltran et al., 2007 at ~3.0–2.9 Ma; Beltran et al., 2011 at 4.66–4.38 Ma; Herbert et al., 2015 at ~3.5–1.5 Ma; Plancq et al., 2015 at 3.6–2.6 Ma). Our SST reconstruction from the PSS section provides the first continuous record from the Eastern Mediterranean over the c. 4.1–3.25 Ma interval (Fig. 6a).

Virtually all sapropels (S56–S94) in the PSS record were deposited under warmer conditions (mean SST: 26.6 °C) compared to the grey marly intervals (mean SST: 25.7 °C) (Fig. 6a). This is in agreement with previous studies of Pliocene sequences in Sicily (mean SST 26.1–26.4 °C; Fig. 6b, c). Consistently warmer conditions found in sapropel layers reflect NH insolation maxima (Emeis et al., 1998; Herbert et al., 2015), linked to the Earth's precession cycle (Hilgen, 1991a, 1991b). Spectral analysis of PSS sapropel cycles matches this 21–23 kyr 'bundling cyclicity' (Athanasiou et al., 2015). Pliocene sapropels in both central (Beltran et al., 2011; Herbert et al., 2015; Plancq et al., 2015) and Eastern (this study) Mediterranean were deposited under much warmer conditions than the most recent sapropel S1 at 10–6 ka BP (~19–23 °C, e.g., Emeis et al., 2000b; Gogou et al., 2007; Triantaphyllou et al.,

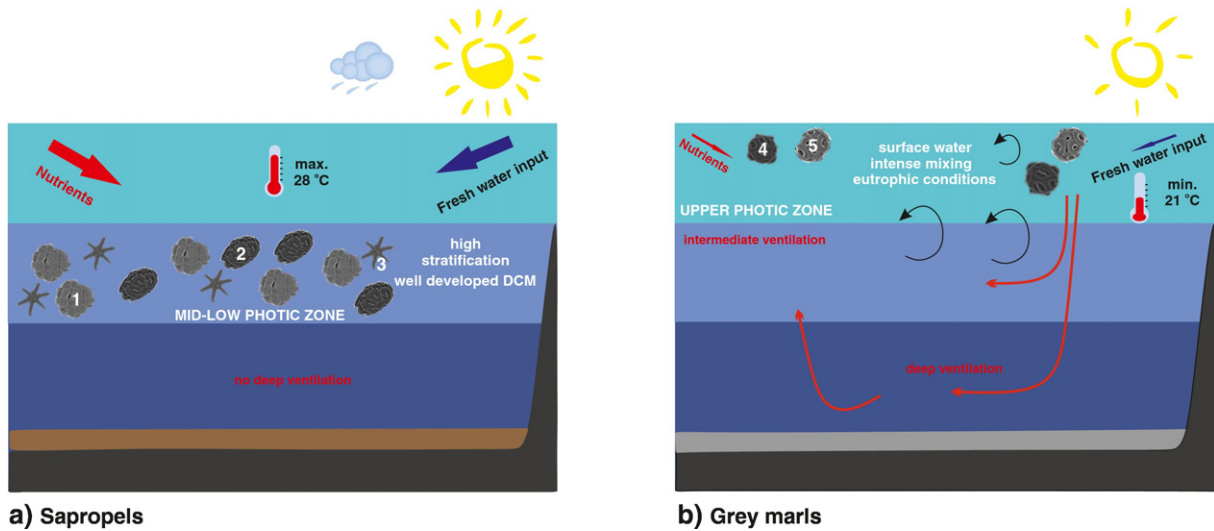| lithology	calcareous nannofossil species indicators		geochemical / environmental evidence	Water column structure	Palaeoceanographic conditions
	F. profunda *Helicosphaera* spp. *Discoaster* spp. *P. lacunosa*	small *Reticulofenestra* spp. small *Gephyrocapsa* spp. *Umbilicosphaera jafari*	OC U_{37}^{K} SST S-index		
A (sapropels)	↑	↓	↑	high stratification-shoaling of the pycnocline productivity in the mid-low photic zone-DCM preservation of organic matter	warm/oligotrophic high fresh water input bottom dysoxia/anoxia
B (grey marls)	↓	↑	↓	surface water productivity	cooler/eutrophic intense surface water mixing

Fig. 5. Schematic representation of the environmental conditions and the mechanisms responsible for the formation of the PSS sapropels (Lithology A) and grey marls (Lithology B). Numbers 1–5 on the figure correspond to *Florisphaera profunda*, *Helicosphaera* spp., *Discoaster* spp., small *Gephyrocapsa* spp. and small *Reticulofenestra* spp. respectively.

2009, 2016). This highlights increased seasonal insolation and land–sea heating contrasts during the Pliocene (Herbert et al., 2015; Plancq et al., 2015).

The warm Pliocene depicted in our PSS record is punctuated by three distinct SST minima at ~3.9 Ma (22.8 °C), 3.58 Ma (22 °C), and between ~3.34 and 3.31 Ma (23.2–23.7 °C) (Fig. 6). The cold MIS Gi20 that marks the pronounced early Pliocene ice volume expansion around 4.0 Ma in the global LR04 stack (Lisiecki and Raymo, 2005), is much weaker in our SST record (Fig. 6a). The SST minimum at ~3.9 Ma reflects the cold MIS Gi16 (Fig. 6a), a rather prominent cooling in the Mediterranean $\delta^{18}O$ stacked record (Wang et al., 2010; Fig. 6d), while the cooling detected at ~3.58 M (Fig. 6a), corresponds to MIS MG12, both in Mediterranean and LR04 stacks (Fig. 6d, e). Our SST record does not capture the major coolings corresponding to MIS Gi2 and Gi4 events (Lisiecki and Raymo, 2005) due to low sampling resolution.

The prevalence of lower SST at ~3.34–3.31 Ma (Fig. 6a) imprint the Mammoth cooling that has been reported to represent the glacial MIS M2 (3.3 Ma; Lisiecki and Raymo, 2005; De Schepper et al., 2013, 2014). The exact nature of the MIS M2 remains enigmatic; large amplitude observed in the oxygen isotope values (Lisiecki and Raymo, 2005), along with the global sea level curve (e.g., Miller et al., 2011), suggest the potential for a major sea level fall, thus implying a build-up of continental ice sheets in the Northern Hemisphere and/or an expansion of the Southern Hemisphere ice. Interestingly, our record reveals bracketing of the glacial MIS M2 (two anomalous precessionally-paced cold cycles) by the

deposition of sapropel cycles 89 and 91 (Fig. 6a). In striking accordance, a similar two-fold saw-tooth shape of the cold MIS M2 has been reported in the Mediterranean stack (Wang et al., 2010) and in the central Mediterranean CRCS record (Herbert et al., 2015; Fig. 6b). Our new SST record therefore confirms that the previously reported cooling ~3.34–3.31 Ma in the Mediterranean (Herbert et al., 2015) is a regionally coherent feature across the central and eastern basins. The simultaneous increase of the lower and mid photic zone dwellers *F. profunda* and *Helicosphaera* spp. and the concomitant high values of the S-index in a stratified depositional environment with increased fresh water input at this time (Figs. 2, 5), support our evidence for a mild expression of the Mammoth cooling event in the Eastern Mediterranean.

Peak cooling during M2 in the central Mediterranean SST record is reported at ~3.34 Ma (Herbert et al., 2015) whereas highest benthic $\delta^{18}O$ values in the LR04 stack occur at ~3.3 Ma (Lisiecki and Raymo, 2005). In our Eastern Mediterranean record, peak SST cooling is slightly younger (~3.315) than the central Mediterranean. Under-sampling of the record possibly aliased away the earlier ~3.34 Ma timing of coldest conditions during MIS M2 at PSS. If the Mammoth cooling event reported here, and more widely across the Mediterranean, is an expression of the globally recognized MIS M2 episode, then the higher fidelity (precessionally-controlled) nature of Pliocene Mediterranean age models provides a slightly older, ~40 kyrs, timing for this event relative to that suggested by the age model of the LR04 (Lisiecki and Raymo, 2005).
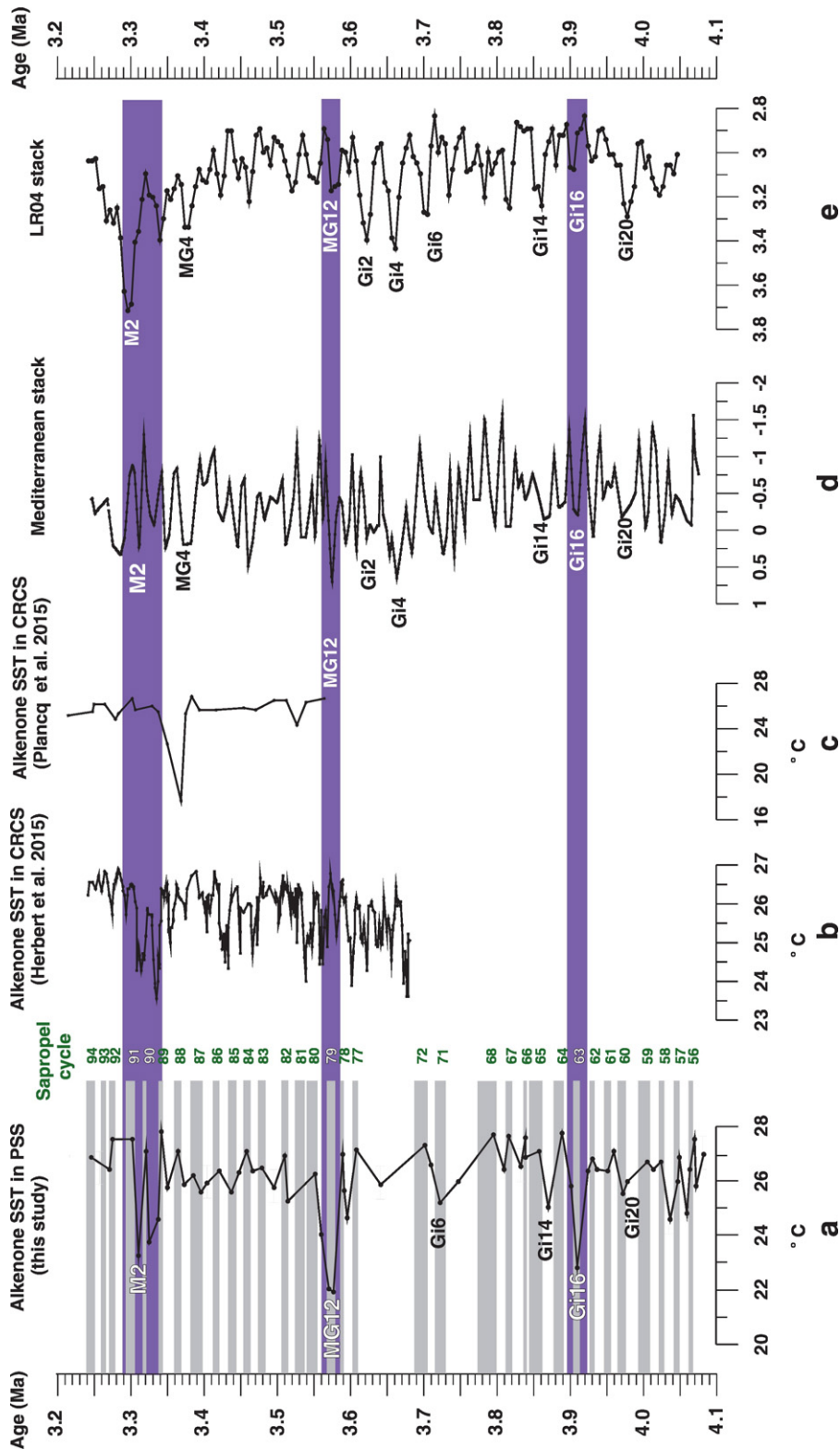
Fig. 6. a. Alkenone derived SST in PSS (this study), b. alkenone derived-SST in CRCS (Herbert et al., 2015), c. alkenone derived-SST in CRCS (Plancq et al., 2015), d. Mediterranean δ¹⁸O stacked record (Wang et al., 2010), e. global marine δ¹⁸O LR04 stack (Lisiecki and Raymo, 2005). The three distinct SST minima are marked with purple bands.

5. Concluding remarks

We presented the first continuous Pliocene alkenone-SST record from the Eastern Mediterranean (island of Cyprus) that documents in detail the warm conditions (mean ~ 26 °C) over the ~4.1–3.25 Ma

"warm Pliocene" interval. Our new SST record captures three cooling events at ~3.91, 3.58 and 3.34–3.31 Ma corresponding to the global MIS Gi16, MG12 and M2 cold periods, respectively. It further demonstrates that the ~3.34–3.31 cooling (MIS M2) previously reported in the central Mediterranean (Herbert et al., 2015) is a coherent regional

feature. Its earlier occurrence in the Mediterranean records with respect to the age attributed by the global LR04 stack (Lisiecki and Raymo, 2005) can either be considered as only a central and Eastern Mediterranean marginal basin signal, or that Mediterranean and LR04 age models discrepancies exist during our study interval.

Comparison of alkenone patterns with the coregistered patterns of calcareous nannofossil assemblages (Noelaerhabdaceae) suggests *P. lacunosa* as the main alkenone contributor in sapropel layers; contribution of *Reticulofenestra* spp. to the overall alkenone production cannot be excluded.

Environmental conditions during the deposition of Pliocene sapropels in the Eastern Mediterranean appear to be similar to those reported for Quaternary sapropels (Grelaud et al., 2012; Rohling et al., 2015). They involve strongly stratified water column conditions and increased productivity in the lower photic zone (development of DCM). The absence of DCM indicators in the central Mediterranean Pliocene records underscores the highly sensitive response of the eastern basin (notably in the proximity of the LIW formation) to strong hydrological changes due to enhanced freshwater discharges induced by insolation-controlled intensification of the African monsoon during times of sapropel deposition.

Acknowledgments

References

Athanasiou, M., Triantaphyllou, M.V., Dimiza, M.D., Gogou, A., Theodorou, G., 2015. Zanclean/Piacenzian transition on Cyprus (SE Mediterranean): calcareous nannofossil evidence of sapropel formation. Geo-Mar. Lett. 35, 367–385.

Backman, J., Raffi, I., Rio, D., Fornaciari, E., Pälike, H., 2012. Biozonation and Biochronology of Miocene through Pleistocene Calcareous Nannofossils from Low and Middle Latitudes. Newsletters on StratigraphyGebrüder Borntraeger, Stuttgart, Germany (http://dx.doi.org/10.1127/0078-0421/2012/0022).

Bailey, I., Hole, G.M., Foster, G.L., Wilson, P.A., Storey, C.D., Trueman, C.N., Raymo, M.E., 2013. An alternative suggestion for the Pliocene onset of major northern hemisphere glaciation based on the geochemical provenance of North Atlantic Ocean ice-rafted debris. Quat. Sci. Rev. 75, 181–194.

Bairbakhish, A.N., Bollmann, J., Sprengel, C., Thierstein, H.R., 1999. A technique for disintegration of aggregates and coccospheres in sediment trap samples. Mar. Micropaleontol. 37, 218–223.

Balco, G., Rovey II, C.W., 2010. Absolute chronology for major Pleistocene advances of the Laurentide Ice Sheet. Geology 38, 795–798.

Bartoli, G., Hönisch, B., Zeebe, R.E., 2011. Atmospheric CO_2 decline during the Pliocene intensification of Northern Hemisphere glaciations. Paleoceanography 26, PA4213.

Beaufort, L., de Garidel-Thoron, T., Mix, A.C., Pisias, N.G., 2001. ENSO-like forcing on oceanic primary production during the late Pleistocene. Science 293, 2440–2444.

Becker, J., Lourens, L.J., Raymo, M.E., 2006. High-frequency climate linkages between the North Atlantic and the Mediterranean during marine oxygen isotope stage 100 (MIS100). Paleoceanography 21. http://dx.doi.org/10.1029/2005PA001168.

Beltran, C., de Rafélis, M., Minoletti, F., Renard, M., Sicre, M.A., Ezat, U., 2007. Coccolith $\delta^{18}O$ and alkenone records in middle Pliocene orbitally controlled deposits: high frequency temperature and salinity variations of sea surface water. Geochem. Geophys. Geosyst. 8. http://dx.doi.org/10.1029/2006GC001483.

Beltran, C., Flores, J.A., Sicre, M.A., Baudin, F., Renard, M., de Rafélis, M., 2011. Long chain alkenones in the early Pliocene Sicilian sediments (Trubi Formation-Punta di Maiata section): implications for the alkenone paleothermometry. Palaeogeogr. Palaeoclimatol. Palaeoecol. 308:253–263. http://dx.doi.org/10.1016/j.palaeo.2011.03.017.

Béthoux, J.P., 1993. Mediterranean sapropel formation, dynamic and climatic viewpoints. Oceanol. Acta 16, 127–133.

Bolton, C.T., Lawrence, K.T., Gibbs, S.J., Wilson, P.A., Cleaveland, L.C., Herbert, T.D., 2010. Glacial–interglacial productivity changes recorded by alkenones and microfossils in late Pliocene eastern equatorial Pacific and Atlantic upwelling zones. Earth Planet. Sci. 295, 401–411.

Bouloubassi, I., Guehenneux, G., Rullkötter, J., 1998. Biological marker significance of organic matter origin and transformation in sapropels from the Mediterranean Ridge, site 969. In: Emeis, K.-C., Robertson, A.H.F., Richter, C., Camerlenghi, A. (Eds.), Proc. ODP, Sci. Res. Ocean Drilling Program Vol. 160, pp. 261–270.

Bouloubassi, I., Rullkötter, J., Meyers, P.A., 1999. Origin and transformation of organic matter in Pliocene-Pleistocene Mediterranean sapropels: organic geochemical evidence reviewed. Mar. Geol. 153, 177–197.

Boussetta, S., Bassinot, F., Sabbatini, A., Caillon, N., Nouet, J., Kallel, N., Rebaubier, H., Klinkhammer, G., Labeyrie, L., 2011. Diagenetic Mg-rich calcite in Mediterranean sediments: quantification and impact on foraminiferal Mg/Ca thermometry. Mar. Geol. 280, 195–204.

Bown, P.R., Young, J.R., 1997. Mesozoic calcareous nannoplankton classification. J. Nanopart. Res. 19, 21–36.

Bown, P.R., Young, J.R., 1998. Techniques. In: Bown, P.R. (Ed.), Calcareous Nannofossil Biostratigraphy. Chapman and Hall, Kluwer Academic, pp. 16–28.

Brassell, S.C., Dumitrescu, M., ODP Leg 198 Shipboard Scientific Party, 2004. Recognition of alkenones in a lower Aptian porcellanite from the west-central Pacific. Org. Geochem. 35, 181–188.

Brassell, S.C., Eglinton, G., Marlowe, I.T., Pfaumann, U., Sarnthein, M., 1986. Molecular stratigraphy: a new tool for climatic assessment. Nature 320, 129–133.

Brigham-Grette, J., Melles, M., Minyuk, P., Andreev, A., Tarasov, P., DeConto, R., Koenig, S., Nowaczyk, N., Wennrich, V., Rosén, P., Haltia, E., Cook, T., Gebhardt, C., Meyer-Jacob, C., Snyder, J., Herzschuh, U., 2013. Pliocene warmth, polar amplification, and stepped Pleistocene cooling recorded in NE Arctic Russia. Science 340, 1421–1427.

Cacho, I., Grimalt, J.O., Pelejero, C., Canals, M., Sierro, F.J., Flores, J.A., Shackleton, N., 1999. Dansgaard–Oeschger and Heinrich event imprints in Alboran Sea paleotemperatures. Paleoceanography 14, 698–705.

Cacho, I., Grimalt, J.O., Canals, M., Sbaffi, L., Shackleton, N.J., Schönfeld, J., Zahn, R., 2001. Variability of the western Mediterranean Sea surface temperature during the last 25,000 years and its connection with the Northern Hemisphere climatic changes. Paleoceanography 16, 40–52.

Casford, J.S.L., Rohling, E.J., Abu-Zied, R.H., Fontanier, C., Jorissen, F.J., Leng, M.J., Schmiedl, G., Thomson, J., 2003. A dynamic concept for Eastern Mediterranean circulation and oxygenation during sapropel formation. Palaeogeogr. Palaeoclimatol. Palaeoecol. 190, 103–119.

Castradori, D., 1993. Calcareous nannofossil and the origin of Eastern Mediterranean sapropels. Paleoceanography 8, 459–471.

Castradori, D., 1998. Calcareous nannofossils in the basal Zanclean of the eastErn Mediterranean Sea: remarks on paleoceanography and sapropel formation. Proc. Ocean Drill. Program Sci. Results 160, 113–123.

Colleoni, F., Masina, S., Negri, A., Marzocchi, A., 2012. Plio-Pleistocene high–low latitude climate interplay: a Mediterranean point of view. Earth Planet. Sci. Lett. 319, 35–44.

Colmenero-Hidalgo, E., Flores, J.A., Sierro, J., Barcena, M.A., Lowemark, L., Schonfeld, J., Grimalt, J.O., 2004. Ocean surface water response to shortterm climate changes revealed by coccolithophores from the Gulf of Cadiz (NE Atlantic) and Alboran Sea (W Mediterranean). Palaeogeogr. Palaeoclimatol. Palaeoecol. 205, 317–336.

Combourieu-Nebout, N., Foucault, A., Mélières, F., 2004. Vegetation markers of palaeoclimate cyclical changes in the Pliocene of Punta Piccola (Sicily, Italy). Palaeogeogr. Palaeoclimatol. Palaeoecol. 214, 55–66.

Conte, M.H., Sicre, M.A., Rühlemann, C., Weber, J.C., Schulte, S., Schulz-Bull, D., Blanz, T., 2006. Global temperature calibration of the alkenone unsaturation index (UK′37) in surface waters and comparison with surface sediments. Geochem. Geophys. Geosyst. 7. http://dx.doi.org/10.1029/2005GC001054.

De Lange, G.J., Thomson, J., Reitz, A., Slomp, C.P., Principato, M.S., Erba, E., Corselli, C., 2008. Synchronous basin-wide formation and redox-controlled preservation of a Mediterranean sapropel. Nat. Geosci. 1, 606–610.

Dermitzakis, M.D., Theodoridis, S.A., 1978. Planktonic foraminifera and calcareous nanoplankton from the Pliocene of Koufonisi Island (East Crete, Greece). Ann. Géol. Pays Hellén. 29, 630–643.

De Schepper, S., Groeneveld, J., Naafs, B.D.A., Van Renterghem, C., Hennissen, J., Head, M.J., Louwye, S., Fabian, K., 2013. Northern Hemisphere glaciation during the globally warm early Late Pliocene. PLoS One 8 (12):81508. http://dx.doi.org/10.1371/JP0081508.

De Schepper, S., Gibbard, P.L., Salzmann, U., Ehlers, J., 2014. A global synthesis of the marine and terrestrial evidence for glaciation during the Pliocene Epoch. Earth-Sci. Rev. 135, 83–102.

Dowsett, H.J., Poore, R., 1991. Pliocene sea surface temperatures of the North Atlantic Ocean at 3.0 Ma. Quat. Sci. Rev. 10, 189–204.

Dowsett, H.J., Robinson, M.M., Haywood, A.M., Hill, D.J., Dolan, A.M., Stoll, D.K., Chan, W.L., Abe-Ouchi, A., Chandler, M.A., Rosenbloom, N.A., Otto-Bliesner, B.L., Bragg, F.J., Lunt, D.J., Foley, K.M., Riesselman, C.R., 2012. Assessing confidence in Pliocene Sea surface temperatures to evaluate predictive models. Nat. Clim. Chang. 2, 365–371.

Dowsett, H.J., Foley, K.M., Stoll, D.K., Chandler, M.A., Sohl, L.E., Bentsen, M., Otto-Bliesner, B.L., Bragg, F.J., Chan, W.-L., Contoux, C., Dolan, A.M., Haywood, A.M., Jonas, J.A., Jost, A., Kamae, Y., Lohmann, G., Lunt, D.J., Nisancioglu, K.H., Abe-Ouchi, A., Ramstein, G., Riesselman, C.R., Robinson, M.M., Rosenbloom, N.A., Salzmann, U., Stepanek, C., Strother, S.L., Ueda, H., Yan, Q., Zhang, Z., 2013. Sea surface temperature of the mid-Piacenzian ocean: a data-model comparison. Sci. Rep. 3, 1–8.

Driever, B.W.H., 1988. Calcareous nannofossil biostratigraphy and paleoenvironmental interpretation of the Mediterranean Pliocene. Utrecht Micropaleontol. Bull. 36, 1–245.

Emeis, K.C., Sakamoto, T., Wehausen, R., Brumsack, H.J., 2000a. The sapropel record of the Eastern Mediterranean Sea — results of Ocean Drilling Program Leg 160. Palaeogeogr. Palaeoclimatol. Palaeoecol. 158, 371–395.

Emeis, K.C., Struck, U., Schulz, H.M., Bernasconi, S., Sakamoto, T., Martinez-Ruiz, F., 2000b. Temperature and salinity of Mediterranean Sea surface waters over the last

16,000 years: constraints on the physical environment of S1 sapropel formation based on stable oxygen isotopes and alkenone unsaturation ratios. Palaeogeogr. Palaeoclimatol. 158, 259–280.

Emeis, K.-C., Schulz, H., Struck, U., Rossignol-Strick, M., Erlenkeuser, H., Howell, M.W., Kroon, D., Mackensen, H., Ishizuka, S., Oba, T., Sakamoto, T., Koizumi, I., 2003. Eastern Mediterranean surface water temperatures and δ18O composition during deposition of sapropels in the late Quaternary. Paleoceanography 18, 1–18.

Emeis, K.C., Schulz, H.M., Struck, U., Sakamoto, T., Doose, H., Erlenkeuser, H., Howell, M., Kroon, D., Paterne, M., 1998. Stable isotope and alkenone temperature records of sapropels from sites 964 and 967: constraining the physical environment of sapropel formation in the Eastern Mediterranean Sea. Proc. Ocean Drill. Program Sci. Results 60, 309–331.

Farrimond, P., Eglinton, G., Brassell, S.C., 1986. Alkenones in Cretaceous black shales, Blake-Bahama Basin, western North Atlantic. Org. Geochem. 10, 897–903.

Fedorov, A.V., Brierley, C.M., Lawrence, K.T., Liu, Z., Dekens, P.S., Ravelo, A.C., 2013. Patterns and mechanisms of early Pliocene warmth. Nature 496, 43–49.

Ferguson, J.E., Henderson, G.M., Kucera, M., Rickaby, R.E.M., 2008. Systematic change of foraminiferal Mg/Ca ratios across a strong salinity gradient. Earth Planet. Sci. Lett. 265, 153–166.

Flores, J.A., Bárcena, M.A., Sierro, F.J., 2000. Ocean-surface and wind dynamics in the Atlantic Ocean off Northwest Africa during the last 140,000 years. Palaeogeogr. Palaeoclimatol. Palaeoecol. 161, 459–478.

Flores, J.A., Sierro, F.J., Filippelli, G.M., Bárcena, M.A., Pérez-Folgado, M., Vázquez, A., Utrilla, R., 2005. Surface water dynamics and phytoplankton communities during deposition of cyclic late Messinian sapropel sequences in the western Mediterranean. Mar. Micropaleontol. 56, 50–79.

Fujiwara, S., Tsuzuki, M., Kawachi, M., Minaka, N., Inouye, I., 2001. Molecular phylogeny of the Haptophyta based on the rbcL gene and sequence variation in the spacer region of the RUBISCO operon. J. Phycol. 37, 121–129.

Gartner, S., 1988. Paleoceanography of the Mid-Pleistocene. Mar. Micropaleontol. 13, 23–46.

Gartner, S., Chow, J., Stanton, R.J., 1987. Late Neogene paleoceanography of the Eastern Caribbean, the Gulf of Mexico, and the eastern equatorial Pacific. Mar. Micropaleontol. 12, 255–304.

Gogou, A., Bouloubassi, I., Lykousis, V., Arnaboldi, M., Gaitani, P., Meyers, P.A., 2007. Organic geochemical evidence of abrupt late glacial-Holocene climate changes in the north Aegean Sea. Palaeogeogr. Palaeoclimatol. Palaeoecol. 256, 1–20.

Gogou, A., Triantaphyllou, M.V., Xoplaki, E., Izdebski, A., Parinos, C., Dimiza, M., Bouloubassi, I., Luterbacher, J., Kouli, K., Martrat, B., Toreti, A., Fleitmann, D., Rousakis, G., Kaberi, H., Athanasiou, M., Lykousis, V., 2016. Climate variability and socio-environmental changes in the northern Aegean (NE Mediterranean) during the last 1500 years. Quat. Sci. Rev. 136, 209–228.

Grauel, A.L., Leider, A., Goudeau, M.L.S., Müller, I.A., Bernasconi, S.M., Hinrichs, K.U., de Lange, G.J., Zonneveld, K.A.F., Versteegh, G.J.M., 2013. What do SST proxies really tell us? A high-resolution multiproxy (UK′ 37, TEXH 86 and foraminifera d18O) study in the Gulf of Taranto, central Mediterranean Sea. Quat. Sci. Rev. 73, 115–131.

Grelaud, M., Marino, G., Ziveri, P., Rohling, E.J., 2012. Abrupt shoaling of the nutricline in response to massive freshwater flooding at the onset of the last interglacial sapropel event. Paleoceanography 27, PA3208. http://dx.doi.org/10.1029/2012PA002288.

Herbert, T.D., 2014. Alkenone paleotemperature determinations. In: Holland, H.D., Turekian, K.K. (Eds.), Treatise on Geochemistry, second ed. Elsevier, Oxford, pp. 399–433.

Herbert, T.D., Ng, G., Peterson, L.C., 2015. Evolution of Mediterranean Sea surface temperatures 3.5–1.5 Ma: regional and hemispheric influences. Earth Planet. Sci. Lett. 409, 307–318.

Hilgen, F.J., 1991a. Extension of the astronomically calibrated (polarity) time scale to the Miocene/Pliocene boundary. Earth Planet. Sci. Lett. 104, 349–368.

Hilgen, F.J., 1991b. Astronomical calibration of Gauss to Matuyama sapropels in the Mediterranean and implication for the geomagnetic polarity time scale. Earth Planet. Sci. Lett. 104, 226–244.

Hilgen, F.J., Abdul Aziz, H., Krijgsman, W., Raffi, I., Turco, E., 2003. Integrated stratigraphy and astronomical tuning of the Serravallian and lower Tortonian at Monte dei Corvi (middle-upper Miocene, northern Italy). Palaeogeogr. Palaeoclimatol. Palaeoecol. 199, 229–264.

Khélifi, N., Sarnthein, M., Andersen, N., Blanz, T., Frank, M., Garbe-Schönberg, D., Haley, B.A., Stumpf, R., Weinelt, M., 2009. A major and long-term Pliocene intensification of the Mediterranean outflow, 3.5–3.3 Ma ago. Geology 37, 811–814.

Kouwenhoven, T.J., Morig, I.C., Negri, A., Giunta, S., Krijgsman, W., Rouchy, J.M., 2006. Paleoenvironmental evolution of the Eastern Mediterranean during the Messinian: constraints from integrated microfossil data of the Pissouri Basin (Cyprus). Mar. Micropaleontol. 60, 17–44.

Krijgsman, W., Blanc-Valleron, M.M., Flecker, R., Hilgen, F.J., Kouwenhoven, T.J., Merle, D., Orszag-Sperber, F., Rouchy, J.M., 2002. The onset of the Messinian salinity crisis in the Eastern Mediterranean (Pissouri Basin, Cyprus). Earth Planet. Sci. Lett. 194, 299–310.

Krom, M.D., Brenner, N.K., Neori, A., Gordon, L.I., 1992. Nutrient dynamics and new production in a warm-core eddy from the Eastern Mediterranean Sea. Deep-Sea Res. 39, 467–480.

Lancis, C., Tent-Manclús, J.E., Flores, J.A., Soria, J.M., 2015. The Pliocene Mediterranean infilling of the Messinian erosional surface: new biostratigraphic data based on calcareous nannofossils (Bajo Segura Basin, SE Spain). Geol. Acta 13, 211–228.

Lang, D.C., Bailey, I., Wilson, P.A., Chalk, T.B., Foster, G.L., Gutjahr, M., 2016. Incursions of southern-sourced water into the deep North Atlantic during late Pliocene glacial intensification. Nat. Geosci. 9, 375–379.

Lisiecki, L.E., Raymo, M.E., 2005. A Pliocene-Pleistocene stack of 57 globally distributed benthic δ18O records. Paleoceanography 20, PA1003.

Lourens, L.J., 2004. Revised tuning of Ocean Drilling Program Site 964 and KC01B (Mediterranean) and implications for the δ18O, tephra, calcareous nannofossil, and geomagnetic reversal chronologies of the past 1.1 Myr. Paleoceanography 19. http://dx.doi.org/10.1029/2003PA000997.

Lourens, L.J., Antonarakou, A., Hilgen, F.J., Van Hoof, A.A.M., Vergnaud-Grazzini, C., Zachariasse, W.J., 1996. Evaluation of the Plio-Pleistocene astronomical timescale. Paleoceanography 11, 391–413.

Lourens, L.J., Hilgen, F.J., Gudjonsson, L., Zachariasse, W.J., 1992. Late Pliocene to early Pleistocene astronomically forced sea surface productivity and temperature variations in the Mediterranean. Mar. Micropaleontol. 19, 49–78.

Malanotte-Rizzoli, P., Manca, B.B., Ribera d'Alcalà, M., Theocharis, A., Brenner, S., Budillon, G., Ozsoy, E., 1999. The Eastern Mediterranean in the 80s and in the 90s: the big transition in the intermediate and deep circulations. Dyn. Atmos. Oceans 29, 365–395.

Malinverno, E., Prahl, F.G., Popp, B.N., Ziveri, P., 2008. Alkenone abundance and its relationship to the coccolithophore assemblage in Gulf of California surface waters. Deep-Sea Res. I 55, 1118–1130.

Marino, M., Maiorano, P., Lirer, F., 2008. Changes in calcareous nannofossil assemblages during the mid-Pleistocene revolution. Mar. Micropaleontol. 69, 70–90.

Marlowe, I.T., Brassell, S.C., Eglinton, G., Green, J.C., 1990. Long-chain alkenones and alkyl alkenoates and the fossil coccolith record of marine sediments. Chem. Geol. 88, 349–375.

Martínez-Botí, M.A., Foster, G.L., Chalk, T.B., Rohling, E.J., Sexton, P.F., Lunt, D.J., Pancost, R.D., Badger, M.P.S., Schmidt, D.N., 2015. Plio-Pleistocene climate sensitivity evaluated using high-resolution CO2 records. Nature 518, 49–54.

Martrat, B., Grimalt, J.O., Lopez-Martinez, C., Cacho, I., Sierro, F.J., Flores, J.A., Zahn, R., Canals, M., Curtis, J.H., Hodell, D.A., 2004. Abrupt temperature changes in the western Mediterranean over the past 250,000 years. Science 306, 1762–1765.

Menzel, D., Hopmans, E.C., van Bergen, P.F., de Leeuw, J.W., Sinninghe Damsté, J.S., 2002. Development of photic zone euxinia in the Eastern Mediterranean basin during deposition of Pliocene sapropels. Mar. Geol. 189, 215–226.

Menzel, D., van Bergen, P.F., Schouten, S., Sinninghe Damsté, J.S., 2003. Reconstruction of changes in export productivity during Pliocene sapropel deposition: a biomarker approach. Palaeogeogr. Palaeoclimatol. Palaeoecol. 190, 273–287.

Miller, K.G., Mountain, G.S., Wright, J.D., Browning, J.V., 2011. A 180-million-year record of sea level and ice volume variations from continental margin and deep-sea isotopic records. Oceanography 24, 40–53.

Molfino, B., McIntyre, A., 1990. Precessional forcing of nutricline dynamics in the equatorial Atlantic. Science 249, 766–769.

Moreno, A., Perez, A., Frigola, J., Nieto-Moreno, V., Rodrigo-Gamiz, M., Martrat, B., Gonzalez-Samperiz, P., Morellon, M., Martín-Puertas, C., Corella, J.P., Belmonte, A., Sancho, C., Cacho, I., Herrera, G., Canals, M., Grimalt, J.O., Jimenez-Espejo, F., Martínez-Ruiz, F., Vegas-Vilarrúbia, T., Valero-Garces, B.L., 2012. The Medieval Climate Anomaly in the Iberian Peninsula reconstructed from marine and lake records. Quat. Sci. Rev. 43, 16–32.

Müller, P.J., Čepek, M., Ruhland, G., Schneider, R.R., 1997. Alkenone and coccolithophorid species in late Quaternary sediments from the Walvis Ridge: implications for the alkenone paleotemperature method. Palaeogeogr. Palaeoclimatol. Palaeoecol. 135, 71–96.

Müller, P.J., Kirst, G., Rulhand, G., von Storch, I., Rosell-Melé, A., 1998. Calibration of the alkenone paleotemperature index based on core-tops from the Eastern South Atlantic and the global ocean (60°N-60°S). Geochim. Cosmochim. Acta 62, 1757–1772.

Myers, P.G., Haines, K., Rohling, E.J., 1998. Modeling the paleocirculation of the Mediterranean: the last glacial maximum and the Holocene with emphasis on the formation of sapropel S1. Paleoceanography 13, 586–606.

Negri, A., Morigi, C., Giunta, S., 2003. Are productivity and stratification important to sapropel deposition? Microfossil evidence from late Pliocene insolation cycle 180 at Vicra, Calabria. Palaeogeogr. Palaeoclimatol. Palaeoecol. 190, 243–255.

Nieto-Moreno, V., Martínez-Ruiz, F., Willmott, V., García-Orellana, J., Masque, P., Sinninghe Damste, J.S., 2013. Climate conditions in the westernmost Mediterranean over the last two millennia: an integrated biomarker approach. Org. Geochem. 55, 1–10.

Okada, H., Honjo, S., 1973. The distribution of ocean coccolithophorids in the Pacific. Deep-Sea Res. 20, 355–374.

Perch-Nielsen, K., 1985. Cenozoic calcareous nannofossils. In: Bolli, H.M., Saunders, J.B., Perch-Nielsen, K. (Eds.), Plankton Stratigraphy. Cambridge University Press, pp. 427–555.

Plancq, J., 2015. Identification Des Producteursd'alcénonesdans le Register Sédimentaire du Cénozoïque: Implications Pour l'utilisation Des Proxys de Paléo-température (UK37) et de Paléo-pCO2. PhD thesis. L'universite Claude Bernard Lyon 1, Lyon, France.

Plancq, J., Grossi, V., Henderiks, J., Simon, L., Mattioli, E., 2012. Alkenone producers during late Oligocene–early Miocene revisited. Paleoceanography 27, PA1202. http://dx.doi.org/10.1029/2011PA002164.

Plancq, J., Grossi, V., Pittet, B., Huguet, C., Rosell-Melé, A., Mattioli, E., 2015. Multi-proxy constraints on sapropel formation during the late Pliocene of central Mediterranean (southwest Sicily). Earth Planet. Sci. Lett. 420, 30–44.

Prahl, F.G., de Lange, G.J., Lyle, M., Sparrow, M.A., 1989. Post-depositional stability of long chain alkenones under contrasting redox conditions. Nature 341, 434–437.

Prahl, F.G., Muehlhausen, L.A., Zahnle, D.L., 1988. Further evaluation of long-chain alkenones as indicators of paleoceanographic conditions. Geochim. Cosmochim. Acta 52, 2303–2310.

Rinna, J., Warning, B., Meyers, P.A., Brumsack, H.J., Rullkötter, J., 2002. Combined organic and inorganic geochemical reconstruction of paleodepositional conditions of a Pliocene sapropel from the Eastern Mediterranean Sea. Geochim. Cosmochim. Acta 66, 1969–1986.

Rio, D., Raffi, I., Villa, G., 1990. Pliocene Pleistocene calcareous nanofossils distribution patterns in the Western Mediterranean. Proc. Ocean Drill. Program Sci. Results 107, 513–533.

Rohling, E.J., 1994. Review and new aspects concerning the formation of Eastern Mediterranean sapropels. Mar. Geol. 122, 1–28.

Rohling, E.J., Cane, T.R., Cooke, S., Sprovieri, M., Bouloubassi, I., Emeis, K.C., Schiebel, R., Kroon, D., Jorissen, F.J., Lorre, A., Kemp, A.E.S., 2002. African monsoon variability during the previous interglacial maximum. Earth Planet. Sci. Lett. 202, 61–75.

Rohling, E.J., Gieskes, W.W.C., 1989. Late Quaternary changes in Mediterranean intermediate water density and formation rate. Paleoceanography 4, 531–545.

Rohling, E.J., Hilgen, F.J., 1991. The Eastern Mediterranean climate at times of sapropel formation: a review. Geol. Mijnb. 70, 253–264.

Rohling, E.J., Marino, G., Grant, K.M., 2015. Mediterranean climate and oceanography, and the periodic development of anoxic events (sapropels). Earth-Sci. Rev. 143, 62–97.

Rossignol-Strick, M., 1985. Mediterranean Quaternary sapropels, an immediate response of the African monsoon to variations of insolation. Palaeogeogr. Palaeoclimatol. Palaeoecol. 49, 237–263.

Rouchy, J.M., Orszag-Sperber, F., Blanc-Valleron, M.M., Pierre, C., Rivière, M., Combourieu Nebout, N., Panayides, I., 2001. Paleoenvironmental changes at the Messinian–Pliocene boundary in the Eastern Mediterranean (Southern Cyprus basins): significance of the Messinian Lago-Mare. Sediment. Geol. 145, 93–117.

Sáez, A.G., Probert, I., Young, J.R., Edvardsen, B., Eikrem, W., Medlin, L.K., 2004. A review of the phylogeny of the Haptophyta. In: Thierstein, H.R., Young, J.R. (Eds.), Coccolithophores: From molecular Processes to Global Impact. Springer-Verlag, Berlin Heidelberg, pp. 251–269.

Seki, O., Foster, G.L., Schmidt, D.N., Mackensen, A., Kawamura, K., Pancost, R.D., 2010. Alkenone and boron-based Pliocene pCO$_2$ records. Earth Planet. Sci. Lett. 292, 201–211.

Stratford, K., Williams, R.G., Myers, P.G., 2000. Impact of the circulation on sapropel formation in the Eastern Mediterranean. Glob. Biogeochem. Cycles 14, 683–695.

Takahashi, K., Okada, H., 2000. Environmental control on the biogeography of modern coccolithophores in the southeastern Indian Ocean offshore of Western Australia. Mar. Micropaleontol. 39, 73–86.

Theocharis, A., Krokos, G., Velaoras, D., Korres, G., 2014. An internal mechanism driving the alternation of the Eastern Mediterranean dense/deep water sources. Geophys. Monogr. 202, 113–137.

Thierstein, H.R., Geitzenauer, K.R., Molfino, B., 1977. Global synchroneity of late Quaternary coccolith datum levels: validation by oxygen isotopes. Geology 5, 400–404.

Thunell, R., Rio, D., Sprovieri, R., Raffi, I., 1991a. Limestone-marl couplets: origin of the early Pliocene Trubi Marls in Calabria, southern Italy. J. Sediment. Petrol. 61, 1109–1122.

Thunell, R., Rio, D., Sprovieri, R., Vergnaud-Grazzini, C., 1991b. An overview of the post-Messinian paleoenvironmental history of the western Mediterranean. Paleoceanography 6, 143–163.

Triantaphyllou, M.V., 2014. Coccolithophore assemblages during the Holocene climatic optimum in the NE Mediterranean (Aegean and northern Levantine Seas, Greece): paleoceanographic and paleoclimatic implications. Quat. Int. 345, 56–67.

Triantaphyllou, M.V., Antonarakou, A., Dimiza, M., Anagnostou, Ch., 2010. Calcareous nannofossil and planktonic foraminiferal distributional patterns during deposition

of sapropels S6, S5 and S1 in the Libyan Sea (Eastern Mediterranean). Geo-Mar. Lett. 30, 1–13.

Triantaphyllou, M.V., Gogou, A., Bouloubassi, I., Dimiza, M., Kouli, K., Roussakis, G., Kotthoff, U., Emeis, K.-C., Papanikolaou, M., Athanasiou, M., Parinos, K., Ioakim, C., Lykousis, V., 2014. Evidence for a warm and humid Mid-Holocene episode in the Aegean and northern Levantine Seas (Greece, NE Mediterranean). Reg. Environ. Chang. 14, 1697–1712.

Triantaphyllou, M.V., Gogou, A., Dimiza, M.D., Kostopoulou, S., Parinos, K., Rousakis, G., Geraga, M., Bouloubassi, I., Fleitmann, D., Zervakis, V., Velaoras, D., Diamantopoulou, A., Sampatakaki, A., Lykousis, V., 2016. Holocene Climatic Optimum decadal-scale paleoceanography in the NE Aegean (Mediterranean Sea). Geo-Mar. Lett. 31, 51–66.

Triantaphyllou, M.V., Ziveri, P., Gogou, A., Marino, G., Lykousis, V., Bouloubassi, I., Emeis, K.C., Kouli, K., Dimiza, M., Rosell-Mele, A., Papanikolaou, M., Katsouras, G., Nunez, N., 2009. Late Glacial-Holocene climate variability at the south-eastern margin of the Aegean Sea. Mar. Geol. 266, 182–197.

Tzanova, A., Herbert, T.D., Peterson, L., 2015. Cooling Mediterranean Sea surface temperatures during the Late Miocene provide a climate context for evolutionary transitions in Africa and Eurasia. Earth Planet. Sci. Lett. 419, 71–80.

van Raden, U.J., Groeneveld, J., Raitzsch, M., Kucera, M., 2011. Mg/Ca in the planktonic foraminifera *Globorotalia inflata* and *Globigerinoides bulloides* from Western Mediterranean plankton tow and core top samples. J. Microencapsul. 78, 101–112.

Villanueva, J., Flores, J.A., Grimalt, J.O., 2002. A detailed comparison of the U37k' and coccolith records over the past 290k years; implications to the alkenone paleotemperature method. Org. Geochem. 33, 897–905.

Volkman, J.K., Eglinton, G., Corner, E.D.S., Forsberg, T.E.V., 1980. Long-chain alkenes and alkenones in the marine coccolithophorid *Emiliania huxleyi*. Phytochemistry 19, 2619–2622.

Volkman, J.K., Barrett, S.M., Blackburn, S.I., Sikes, E.L., 1995. Alkenones in *Gephyrocapsa oceanica*: implications for studies of paleoclimate. Geochim. Cosmochim. Acta 59, 513–520.

Wang, P., Tian, J., Lourens, L.J., 2010. Obscuring of long eccentricity cyclicity in Pleistocene oceanic carbon isotope records. Earth Planet. Sci. Lett. 290, 319–330.

Waters, J.V., Jones, S.J., Armstrong, H.A., 2010. Climatic controls on late Pleistocene alluvial fans, Cyprus. In: Wilford, D., Nichols, G., Giles, P. (Eds.), Alluvial Fan Research and Management: From Reconstructing Past Environments to Identifying the Contemporary Hazards. Geomorphology 115, pp. 228–251.

Young, J.R., 1990. Size variations of Neogene *Reticulofenestra* coccoliths from Indian Ocean DSDP cores. J. Microencapsul. 9, 71–85.

Young, J.R., 1994. Functions of coccoliths. In: Winter, A., Siesser, W.G. (Eds.), Coccolithophores. Cambridge University Press, Cambridge, pp. 63–82.

Young, J.R., 1998. Neogene. In: Bown, P.R. (Ed.), Calcareous Nannofossil Biostratigraphy. Chapman and Hall, Cambridge, U.K., pp. 225–265.

Young, J.R., Bown, P.R., Lees, J.A., 2014. Nannotax3 Website (http://ina.tmsoc.org/Nannotax3).

Ziveri, P., Baumann, K.-H., Boeckel, B., Bollmann, J., Young, J., 2004. Biogeography of selected Holocene coccoliths in the Atlantic Ocean. In: Thierstein, H.R., Young, Y.R. (Eds.), Coccolithophores from Molecular Processes to Global Impact. Springer, Berlin, pp. 403–428.